



HAL
open science

Atomic force microscope measurement and LCAO-S-2+vdW calculations of contact length between a carbon nanotube and a graphene surface

Mahamoudou Seydou, Yannick J. Dappe, Sophie Marsaudon, Jean-Pierre Aimé, Xavier Bouju, Anne-Marie Bonnot

► To cite this version:

Mahamoudou Seydou, Yannick J. Dappe, Sophie Marsaudon, Jean-Pierre Aimé, Xavier Bouju, et al.. Atomic force microscope measurement and LCAO-S-2+vdW calculations of contact length between a carbon nanotube and a graphene surface. *Physical Review B: Condensed Matter and Materials Physics* (1998-2015), 2011, 83 (4), pp.045410. 10.1103/PhysRevB.83.045410 . hal-01002323

HAL Id: hal-01002323

<https://hal.science/hal-01002323>

Submitted on 23 Apr 2018

HAL is a multi-disciplinary open access archive for the deposit and dissemination of scientific research documents, whether they are published or not. The documents may come from teaching and research institutions in France or abroad, or from public or private research centers.

L'archive ouverte pluridisciplinaire **HAL**, est destinée au dépôt et à la diffusion de documents scientifiques de niveau recherche, publiés ou non, émanant des établissements d'enseignement et de recherche français ou étrangers, des laboratoires publics ou privés.

Atomic force microscope measurements and LCAO- S^2 + vdW calculations of contact length between a carbon nanotube and a graphene surface

M. Seydou*

Laboratoire ITODYS-Université Paris 7-Denis Diderot, Bâtiment Lavoisier, 15 rue Jean Antoine de Baïf, 75205 Paris Cedex 13, France

Y. J. Dappe

Institut de Physique et Chimie des Matériaux de Strasbourg (IPCMS), UMR CNRS 7504, 23 rue du Loess, P.O. Box 43, F-67034 Strasbourg Cedex, France

S. Marsaudon and J.-P. Aimé

Chimie et Biologie des Membranes et des Nano-objets (CBMN), UMR CNRS 5248, 88 Avenue des Facultés, F-33402 Talence Cedex, France

X. Bouju

Centre d'Élaboration de Matériaux et d'Études Structurales (CEMES), Nanosciences Group, UPR CNRS 8011, 29 rue Jeanne-Marvig, P.O. Box 94347, F-31055 Toulouse Cedex 4, France

A.-M. Bonnot

Institut Néel, CNRS, 25 rue des Martyrs, P.O. Box 166, F-38042 Grenoble Cedex 9, France

(Received 5 October 2010; published 21 January 2011)

We present here a combined experimental and theoretical determination of single-walled carbon nanotube interaction with a graphene surface. The nanotubes are grown on an atomic force microscope (AFM) tip, and we proceed to retract-approach, as well as perform frequency-modulation experiments on a graphene surface, to determine the adhesive energy. In the meantime, we have calculated the adhesive energy of various nanotubes on a graphene surface by means of the LCAO- S^2 + vdW formalism, to take into account weak interactions in graphitic materials. Experimental and theoretical results are in good agreement, which allows us to deduce the contact length of the tube on the surface. These results open promising perspectives in near-field surface spectroscopy, combining carbon nanotubes and AFM measurements.

DOI: [10.1103/PhysRevB.83.045410](https://doi.org/10.1103/PhysRevB.83.045410)

PACS number(s): 68.37.Ps, 71.15.Mb, 61.48.De, 61.48.Gh

I. INTRODUCTION

Because of their extraordinary electronic, chemical, and mechanical properties, carbon nanotubes¹ (CNT's) and graphene² have attracted a great deal of interest in the scientific community. Applications are envisioned in very different areas, such as electronics, material, medicine, or biology domains. As an example, nanoelectromechanical systems could incorporate both CNT's and graphene.³ Understanding how carbon nanotubes interact with a flat surface, especially such an interesting one as a graphene sheet, will help to find the best buildings and assembling strategies.⁴ A controlled way to move a nanosized object with respect to another is by using the displacement abilities of an atomic force microscope (AFM). The fine control of the AFM tip position with respect to an adsorbate on a surface allows us to induce lateral and vertical manipulations. Lateral induced displacements have already been demonstrated for single atoms, molecules, and nanostructures with the scanning tunneling microscope^{5–10} (STM) as well as with the AFM.^{11–17} On another hand, there are many fewer mechanical vertical manipulations using STM or AFM capabilities.^{18–21} This is mainly due to the fact that local-probe-based methods are very sensitive to the tip-surface distance, and thus more complicated to handle accurately perpendicular to the surface. Nevertheless, single molecule-force spectroscopy has been carried out by pulling a molecule. The molecule is grafted both at the tip apex and the surface, and the mechanical force signal of the

probe is recorded as a function of the tip-surface separation. Most experiments provide insights into conformations of biomolecules^{22–28} or polymers,^{29–34} but not really on CNT's. In the case of a single CNT, one part lies parallel to the surface whereas the other remains almost vertically attached to the tip, and the curvature radius depends on the applied load and on the tube diameter.^{35–37} Here, the CNT-surface interaction is mainly piloted by van der Waals (vdW) interactions. One can find a natural extension by considering an important number of grafted CNT's on a substrate, leading to vertical CNT arrays.^{38,39} Collective effects enhance the attachment of the CNT's sample on a surface, and complete and strong adhesion can be seen as the summation of low vdW interactions. This effect is responsible for the adhesion of a single gecko seta on almost any surface.⁴⁰

AFM sensitivity is mainly governed by the tip apex geometry, and a high aspect ratio of this apex is required to get a good precision. Single-walled CNT's (SWCNT's) attached to an AFM tip present a smaller diameter, which increases the imaging resolution but may exhibit anomalous nonlinear behavior with instabilities.^{36,41–44} A clear presentation of CNT equipped tips can be found in two recent reviews.^{45,46} An accurate understanding of the nanotube interactions with samples is therefore needed.⁴⁷ Moreover, since this interaction is weak or vdW-like, its complete study can be useful to develop new highly sensitive probes on surfaces. By frequency modulation in atomic force microscopy (FM-AFM), Bernard *et al.*⁴⁸ measured the elastic and adhesive energies per cycle

for a carbon nanotube interacting with a graphite surface. They found that the behavior of the nanotube is governed by a competition between the proper elastic energy of the tube and its adhesive interaction with the surface. Of course, the adhesive energy depends strongly on the length of contact between the nanotube and the surface. By using a simple analytical cylinder-plane model⁴⁹ for the interaction force, they determined the contact length of both single-walled and multiwalled carbon nanotubes on a graphite surface and obtained a value around 6 nm for SWCNT's. Also, Strus *et al.* developed a new method in atomic force microscopy called peeling force spectroscopy.⁵⁰ This technique allows us to measure the adhesive energy of a multiwalled nanotube or nanofiber on a surface. They succeeded in separating the components of elastic and interfacial energy for multiwalled nanotubes and nanofibers.⁵⁰ They also identified how the CNT may interact by pinning or slipping with the surface during the intermittent contact regime of the AFM.³⁷ González *et al.* presented a combined experimental and theoretical study of the interaction between a tip and SWCNT's lying on a SiO₂ surface. Adhesion and jump-to-contact forces (JC) are measured in a high vacuum system for SWCNT's with diameters ranging from 1.4 to 4.5 nm. They found adhesion and JC forces of, respectively, 3.2 and 2.4 nN.⁵¹ Regarding the interaction between a CNT and graphene, Kis *et al.*⁵² measured interlayer force between walls in a multiwalled carbon nanotube. They obtained a total dissipation per cycle lower than 0.4 meV/atom. AFM force spectroscopy has also been used to measure the spring constant of a single molecule or a molecular complex⁵³ with forces ranging from 0.5 to 2.5 nN. Recently, using atomic force microscopy based on single molecular force spectroscopy, Zhang *et al.*⁵⁴ measured directly the π - π interaction between a pyrene molecule and graphite. They obtained an interaction force of 55 pN corresponding to a binding energy of 270 meV, that is, ~ 17 meV per carbon atom. From a theoretical point of view, there has been no calculation done on the interaction of a SWCNT with graphene by means of an AFM tip. The reason for this is that such weak interactions that rule these processes cannot be determined accurately by means of standard *ab initio* techniques such as density-functional-theory local-density approximation (DFT-LDA). In a recent paper, we used molecular mechanics calculations with MM + force field to investigate the interaction between a CNT and a graphene surface.⁵⁵ By moving a CNT on a graphene surface in several directions, and calculating the adhesive energy and barrier heights, we observed some situations of trapping and sliding that correspond to thermal noise measurements.

Using a quantum-mechanical approach augmented by an intertube Lennard-Jones potential, Surjan *et al.*⁵⁶ computed the interaction of several families of CNT's with diameters close to the (10,10) tube. Depending on the stacking between tubes, they obtained a rotation barrier in the range 3.9–29.3 meV/Å. The other Lennard-Jones-like method is the one proposed by Girifalco and Ladd,⁵⁷ which gives a theoretical graphene sheet exfoliation energy of 43 meV/atom. On the other hand, a complete N -body calculation of the C₆₀ dispersion energy on graphite gives a value of 16 meV/atom.⁵⁸ In the same spirit, a study considering a (6,0) CNT located 3.4 Å from a graphene sheet gives an indicative adsorption energy of ~ 64 meV/Å or 11 meV/atom. The discrepancy arises from the fact that the

adsorption energy is not calculated at the optimal distance (around 2.8 Å). Moreover, these methods are semiempirical and require some fitted parameters, preventing a good comparison with accurate experimental measurements. The major difficulty in these weakly interacting systems lies in the nonlocal and long-range character of these interactions. Nevertheless, some attempts have been made to overcome this difficulty in the frame of DFT or quantum chemistry methods. For example, the work on the second-order Möller-Plesset theory (MP2) (Refs. 59 and 60) yielded good results but cannot be applied to big systems like CNT's due to the high computational requirements. Similarly, the functional proposed by Lundqvist *et al.*^{61,62} has limitations with regard to the size of the system.

In this work, we use a combined intermolecular perturbation theory and DFT treatment^{63,64} to calculate accurately the binding energy of various SWCNT's on a graphene surface. Then we compare these energies to the one obtained by AFM measurements in contact and dynamic frequency-modulation modes for the same system. The aim of this work is thus to make a significant contribution to the understanding of a SWCNT as a superprobe on an AFM tip by considering as a first example its interaction with a graphene surface.

II. EXPERIMENTS

Our objective here is to determine the interaction energy between a SWCNT and a graphene sheet by means of AFM measurements. We use a SWCNT grown directly on a silicon AFM tip and we measure the force between this system and the graphene sheet by approaching and retracting the tip. These contact mode measurements are carried out in air, at room temperature, on an MFP3D Asylum Research instrument. We use MikroMasch CsC38 and Nanoworld CNT cantilevers with stiffness from 10 to 200 pN/m, resonance frequency in the range 10–40 kHz, and the quality factors Q around 40–70 in air far from the surface. SWCNT's are grown following a standard high filament chemical vapor deposition (HFCVD) method.^{65,66} The diameters of these carbon nanotubes are measured by high-resolution Raman spectroscopy and estimated to be around 1–2 nm.^{67,68} The surface is a graphene layer grown on SiC(100) or highly ordered pyrolytic graphite.

Contact mode force curves and dynamic FM approach-retract curves have been made in air. In contact mode, the piezodisplacement and the corresponding cantilever deflection are recorded during the approach of the CNT to the surface. The adhesion energy corresponds to the area between the force curve and the zero-force axis. Details of the experimental FM mode have been described previously.⁴⁸ In FM mode, the cantilever frequency shift and the damping signal are recorded. Bearing in mind that the damping signal is proportional to the tip-cantilever oscillator dissipation, it is thus related to the energy E dissipated by the oscillating system. This total dissipated energy has two terms: E_0 , which corresponds to the energy required to maintain the oscillation, and the nanotube dissipation due to surface interaction $E_{\text{int}} = E - E_0$. In the absence of friction, the interaction signal becomes equal to the adhesive energy. We present an accurate description of the adhesion energy of a SWCNT on a graphene sheet by means of the DFT-based calculations described in the following section. We have to say, however, that these calculations

constitute only an estimate of the experimental adhesion energy. Indeed, the complex shape of the approach and retract curves shows that the adsorption-desorption process includes a considerable amount of configurational changes, which are obviously not included in the binding energy calculated here. Nevertheless, we will show a rather good agreement between these calculations and the experimental data.

III. CALCULATIONS

The adhesive energy of SWCNT on graphene has been described theoretically using the LCAO- $S^2 + \text{vdW}$ formalism, previously developed and tested in the case of rare-gas dimers,⁶⁹ graphene-graphene interaction,^{63,70} and CNT-CNT lateral interaction.⁶⁴ This formalism takes into account two opposite contributions that aim to describe the weak interaction between the CNT and the graphene plane. The first contribution, which we call chemical energy, is due to the small overlaps between electronic densities of CNT's and graphene, which lead to a net repulsive energy. The second contribution corresponds to the pure vdW interaction due to charge fluctuations in the interacting subsystems. These charge fluctuations are expressed by electronic dipoles, whose interaction is treated in perturbation theory. In this formalism, the SWCNT and the graphene plane are treated separately by means of the DFT code FIREBALL.⁷¹⁻⁷⁴ This code uses a self-consistent version of the Harris functional⁷³ instead of the traditional Kohn-Sham functional based on the electronic density, and an optimized atomiclike orbital basis set.⁷⁵ Finally, we mention that pseudopotentials are used in the FIREBALL calculations,^{76,77} and that the LDA exchange-correlation energy is calculated using the multicenter weighted exchange-correlation density approximation (McWEDA).^{72,74} This preliminary step will give access to the intrinsic characteristics of each subsystem as well as their energy spectrum. In the following step, atomic dipoles, electronic density overlaps, and hoppings are evaluated to calculate the weak interactions between the SWCNT in perturbation theory and within the dipolar approximation. Since we want to compare these results with AFM measurements, we have calculated the interaction energy of several SWCNT's with a graphene sheet, such as the (5,5), (6,0), (8,0), and (10,0), whose corresponding diameters, inside the experimental range, are, respectively, 6.8, 4.7, 6.3, and 13.0 Å. The SWCNT/graphene system has been modeled considering an elementary slice of a SWCNT in interaction with a nanoribbon of graphene. This elementary cell is then repeated periodically along the axis of the SWCNT as well as in the lateral directions. The nanoribbon has been chosen large enough to minimize interactions with SWCNT's of the neighboring cells. The adsorption energy is calculated as a function of the SWCNT-surface distance at a fixed orientation, which seems reasonable considering the physisorption state of the SWCNT and thus the very small deformation of the overall structure.

IV. RESULTS AND DISCUSSIONS

In this section, we will present combined experimental and theoretical results of SWCNT interaction on graphene. The force curve for the SWCNT-tip approach and retraction on graphene is represented in Fig. 1.

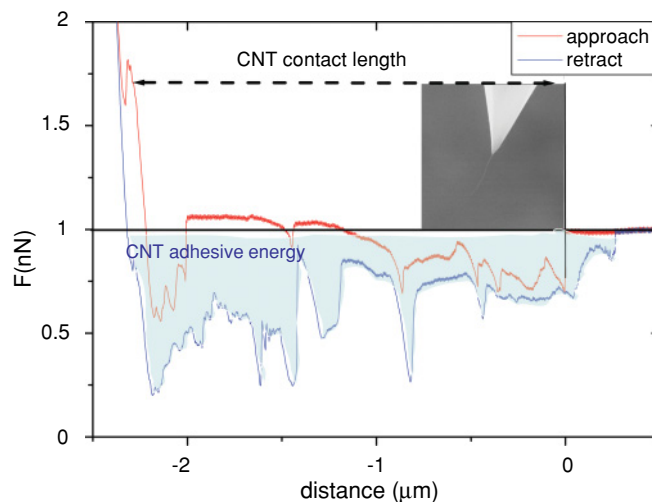


FIG. 1. (Color online) Approach and retract curve for SWCNT labeled 1. As is usual for a soft long SWCNT, the curves present multiple transitions. Experimental energy of adhesion is represented by the shaded surface. Inset: a scanning electron microscope (SEM) image of the SWCNT adsorbed on the tip.

We represent a typical approach-retract curve around the interest zone corresponding to the SWCNT fingerprint. Those curves are characteristic of one SWCNT, with different domains that correspond to the different conformations of SWCNT during approach and retraction. The distance between the SWCNT contact position on the surface and the position where the Si tip signature appears is considered to be the contact length of the SWCNT. The adhesive energy is evaluated as the area between the retract curve and the axis $F(d) = 0$ along the SWCNT fingerprint region.

Measured adhesive energy and contact length of several SWCNT's on graphene are reported in Table I. The experimental energy normalized by the contact length is then compared to the theoretical adhesive energies. The adhesive energy per unit length varies strongly with the contact length. For example, we obtained 0.47, 0.38, 0.44, 0.14, and 0.13 eV/Å, respectively, for SWCNT's labeled 1, 2, 3, 4, and 5 in Table I. The values are higher for the short SWCNT's labeled 1^a and 6. The SWCNT labeled 1^a corresponds to the SWCNT labeled 1 after a first imaging. As with standard tips in near-field spectroscopies, the nanotube breaks on the surface during imaging. In the present case, the SWCNT 1 has

TABLE I. Experimental adhesive energies and contact lengths of SWCNT's deduced from approach-retract curves. The SWCNT labeled 1^a is the same as the one labeled 1, but after imaging, the length is reduced from 2400 to 39 nm (see text).

CNT	Contact length (nm)	E_{adh} (eV)	E (eV/Å)
1	2400	11294	0.47
1 ^a	39	648	1.66
2	130	492	0.38
3	1000	4383	0.44
4	550	749	0.14
5	392	501	0.13
6	30	476	1.58

TABLE II. Calculated adhesive energies obtained for different SWCNT diameters.

SWCNT	Diameter (nm)	E_{adh} (eV/Å)
(6,0)	0.47	0.21
(8,0)	0.63	0.23
(5,5)	0.68	0.33
(10,10)	1.30	0.47

been reduced from 2400 to 39 nm, giving us the opportunity to study the interaction with a much shorter nanotube. Our results are in good agreement with theoretical calculations for significant contact length (Table II) and disagree for short length. This is the consequence of an important effect of the SWCNT extremity. But this problem can also be turned to an advantage. Indeed, a small modification of the end of the SWCNT can affect considerably the adhesion energy. Therefore, the interaction with a corrugated surface as well as a molecular adsorbate would be reflected in this adhesive energy, converting the tip-SWCNT system in a new highly sensitive probe for nanostructured surfaces. This high sensitivity is mainly due to the smooth vdW-like interaction between SWCNT and the surface.

We now present the results of the LCAO- S^2 + vdW calculations giving in a very accurate way the contact length of the various SWCNT's on the graphene surface. These results are shown in Fig. 2 for the SWCNT (5,5), (6,0), (8,0), and (10,0). The geometry of the system is presented in the inset. The obtained adhesive energies are, respectively, 0.33, 0.21, 0.23, and 0.47 eV/Å.

First, it can be seen trivially that the adhesion energy per unit length increases with the SWCNT diameter, since there are more atoms interacting at the interface. This fact is confirmed by molecular mechanics calculations in which Avouris *et al.*⁷⁸ show a linear dependence between adhesive energy and tube diameter. We can also observe a dependence with the chirality, since metallic SWCNT's bind more strongly with the graphene surface. This is due to the smaller gap, which

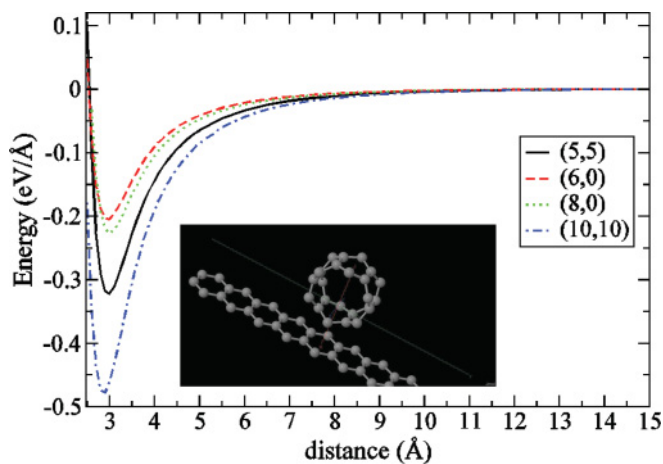


FIG. 2. (Color online) Theoretical adhesive energies for different SWCNT diameters determined in the LCAO- S^2 + vdW model. The unit cell used for the calculation is represented in the inset.

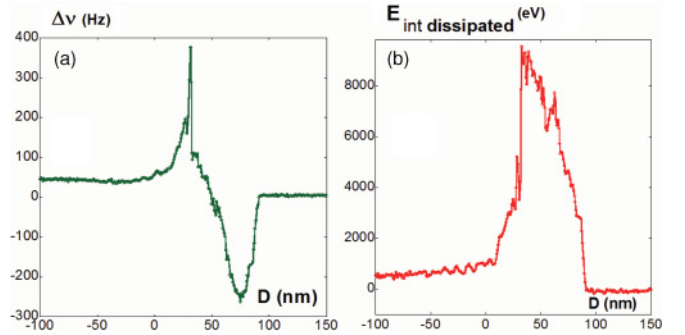


FIG. 3. (Color online) Experimental frequency-modulation mode recorded with SWCNT no. 5: frequency shift (a) and corresponding interaction energy dissipation (b) variation with nanotube-surface distance D recorded during tip approach. The oscillation amplitude is 92 nm. These curves are typical of SWCNT-surface interactions that were modeled previously with a simple analytical model describing SWCNT elasticity and adhesion.⁴⁸ At a distance of 92 nm from the surface, the nanotube starts interacting with the surface. This corresponds to a negative frequency shift and a dissipation jump, associated with the attractive interaction of the tube end, $E_{\text{apex-adh}}$. The nanotube is then in intermittent contact with an increase of repulsive interaction and dissipation. At $D = 32$ nm, the nanotube does not leave the surface with an instantaneous frequency jump. Therefore, the dissipation drops, due to the unsticking of the nanotube end from the surface at each cycle. Consequently, the energy dissipation $E_{\text{apex-adh}}$ due to the SWCNT end vanishes.

has an influence on the transition energies associated with the electronic dipoles.⁶⁴

Now we compare the results obtained in two different modes for the same nanotube: the contact mode, whose value is given in Table I, and the FM mode, whose results are presented in Fig. 3. For the FM mode, the interaction energy is measured in terms of dissipation, stiffness of the cantilever, amplitude, and frequency of oscillations. For these measurements, we use a SWCNT grown on a tip, attached to a lever, with a frequency resonance of 18.6 kHz. The oscillation amplitude is 92 nm and the stiffness is 48 pN/nm. In Fig. 3, we represent the normalized dissipative energy and frequency shift as a function of the piezodisplacement. The contact length is deduced by the distance between the SWCNT and the surface, subtracting the oscillations' amplitude. When the contact length becomes significant (more than 100 nm), the curve can be fitted by a polynomial function. We consider the energy per unit value at 392 nm, which corresponds to the contact measurement with the same SWCNT. We then observe a good agreement between energy values measured from the two modes. In all cases, for small contact length, the energy value is higher, probably because of the SWCNT extremity or because of an effect of the tip, which is obviously closer to the surface in that configuration. A direct comparison between experiment and theory remains complicated since exact experimental values of the SWCNT diameters used here are beyond our knowledge.

For the theoretical calculations, we have considered SWCNT's with different diameters from 0.47 to 1.3 nm, according to the experimental range, and different chiralities, leading to an adhesive energy between 0.21 and

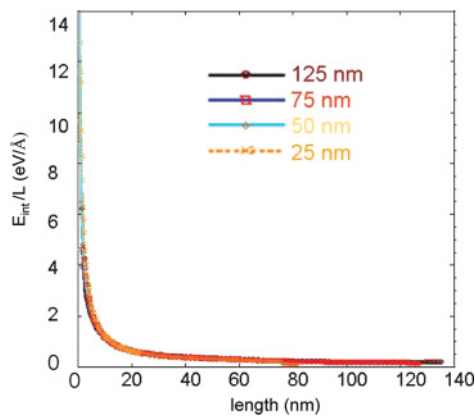


FIG. 4. (Color online) Interaction dissipation energy per unit length for a SWCNT grown on an AFM tip on a stiffer oscillator for four different amplitudes.

0.47 eV/Å. These values are comparable with contact and FM measurements done in ambient conditions. Actually, graphite was always cleaved just before the experiment to maintain the hydrophobic character of the surface. This could explain why the results agree without the need for ultrahigh vacuum for surface-state control. Moreover, even if a thin liquid layer remains on the substrate, one can estimate a screening between 10% and 15% of the vdW contributions^{49,79,80} leading to a decrease of the calculated values in vacuum of only a few tens of a millielectron volt. Such a film would also have an impact on the mechanical response of the tube when it approaches the surface, and the presence of a meniscus would modify the measured force. The coherence between contact and frequency-modulation mode data and the calculated values is rather encouraging, despite the relatively low sensitivity of the measurements due to the low oscillator quality factor of the contact levers. We show in Fig. 4 an additional experimental data set in frequency modulation recorded with a stiffer lever designed for dynamical modes.

Here we represent the dissipated energy versus the contact length between the SWCNT and the graphene surface. This length is determined by the approach of the nanotube to the surface. One important aspect is that the dissipated energy per unit length does not depend on the oscillation amplitude. Moreover, this energy goes asymptotically to the value determined theoretically in our formalism. This result confirms the good agreement between theory and experiments, for significant contact lengths, where the tip effect becomes negligible, as discussed previously.

The agreement between the experimental data and the calculations is really good, taking into account the different environments of both studies (ambient conditions versus vacuum). Such an agreement could motivate us to go further in the comparison and could contribute to the development of long carbon nanotube tips used for surface characterization as initiated by Strus *et al.*^{50,81}

V. SUMMARY

We have determined the adhesion energy of SWCNT on a graphite surface. Both contact and dynamic frequency-modulation modes in AFM lead to the same result for significant contact lengths. Theoretical calculations based on the LCAO- S^2 + vdW formalism give comparable values for the same diameter range as considered experimentally. In this approach, weak and vdW forces are accurately evaluated. For short lengths, side adhesion may not take place, thus the experimental data cannot be compared to the model. For long lengths, the experimental values are coherent with the calculated energies, despite the ambient conditions. This agreement could lead to another use for long carbon nanotube probes as surface sensors.

ACKNOWLEDGMENTS

We thank the ANR P3N for funding the research with the IMPROVE-LM program. Many thanks also to Stephan Roche for discussions on the theoretical part.

*mahamadou.seydou@paris7.jussieu.fr

¹S. Iijima, *Nature (London)* **354**, 56 (1991).

²A. K. Geim and K. S. Novoselov, *Nat. Mater.* **6**, 183 (2007).

³A. Barreiro, R. Rurali, E. R. Hernández, J. Moser, T. Pichler, L. Forró, and A. Bachtold, *Science* **320**, 775 (2008).

⁴C. Soldano, A. Mahmood, and E. Dujardin, *Carbon* **48**, 2127 (2010).

⁵S. Gauthier, *Appl. Surf. Sci.* **164**, 84 (2000).

⁶S.-W. Hla, *J. Vac. Sci. Technol. B* **23**, 1351 (2005).

⁷F. Moresco, *Phys. Rep.* **399**, 175 (2004).

⁸L. Grill, K.-H. Rieder, F. Moresco, G. Rapenne, S. Stojkovic, X. Bouju, and C. Joachim, *Nat. Nanotech.* **2**, 95 (2007).

⁹L. Grill, *J. Phys. Condens. Matter* **20**, 053001 (2008).

¹⁰L. Grill, *J. Phys. Condens. Matter* **22**, 084023 (2010).

¹¹X. Bouju, C. Joachim, and C. Girard, *Phys. Rev. B* **50**, 7893 (1994).

¹²L. Pizzagalli and A. Baratoff, *Phys. Rev. B* **68**, 115427 (2003).

¹³Y. Sugimoto, M. Ane, S. Hirayama, N. Oyabu, O. Custance, and S. Morita, *Nat. Mater.* **4**, 156 (2005).

¹⁴T. Junno, K. Deppert, L. Montelius, and L. Samuelson, *Appl. Phys. Lett.* **66**, 3627 (1995).

¹⁵M. C. Strus, R. R. Lahiji, P. Ares, V. López, A. Raman, and R. Reifengerger, *Nanotechnology* **20**, 385709 (2009).

¹⁶E. Tranvouez, A. Orioux, E. Boer-Duchemin, C. H. Devillers, V. Huc, G. Comtet, and G. Dujardin, *Nanotechnology* **20**, 165304 (2009).

¹⁷E. Gneco, A. Rao, K. Mougín, G. Chandrasekar, and E. Meyer, *Nanotechnology* **21**, 215702 (2010).

¹⁸G. Dujardin, A. Mayne, O. Robert, F. Rose, C. Joachim, and H. Tang, *Phys. Rev. Lett.* **80**, 3085 (1998).

¹⁹L. Pizzagalli, C. Joachim, X. Bouju, and C. Girard, *Europhys. Lett.* **38**, 97 (1997).

²⁰Y. Sugimoto, P. Pou, O. Custance, P. Jelinek, M. Abe, R. Perez, and S. Morita, *Science* **322**, 413 (2008).

²¹L. Lafferentz, F. Ample, H. Yu, S. Hecht, C. Joachim, and L. Grill, *Science* **323**, 1193 (2009).

- ²²E. L. Florin, V. T. Moy, and H. E. Gaub, *Science* **264**, 415 (1994).
- ²³M. Rief, F. Oesterhelt, B. Heymann, and H. E. Gaub, *Science* **275**, 1295 (1997).
- ²⁴H. Clausen-Schaumann, M. Seitz, R. Krautbauer, and H. E. Gaub, *Curr. Opin. Chem. Biol.* **4**, 524 (2000).
- ²⁵M. I. Giannotti and G. J. Vancso, *ChemPhysChem* **8**, 2290 (2007).
- ²⁶S. K. Kufer, E. M. Puchner, H. Gump, T. Liedl, and H. E. Gaub, *Science* **319**, 594 (2008).
- ²⁷S. K. Kufer, M. Strackharn, S. W. Stahl, H. Gump, E. M. Puchner, and H. E. Gaub, *Nat. Nanotech.* **4**, 45 (2009).
- ²⁸S. Kumar and M. S. Li, *Phys. Rep.* **486**, 1 (2010).
- ²⁹T. Senden, J.-M. di Meglio, and P. Auroy, *Eur. Phys. J. B* **3**, 211 (1998).
- ³⁰T. Hugel, N. B. Holland, A. Cattani, L. Moroder, M. Seitz, and H. E. Gaub, *Science* **296**, 1103 (2002).
- ³¹A. Scherer, C. Zhou, J. Michaelis, C. Brauchle, and A. Zumbusch, *Macromolecules* **38**, 9821 (2005).
- ³²M. Bergensträhle, E. Thormann, N. Nordgren, and L. A. Berglund, *Langmuir* **25**, 4635 (2009).
- ³³Q.-Z. Yang, Z. Huang, T. J. Kucharski, D. Khvostichenko, J. Chen, and R. Boulatov, *Nat. Nanotech.* **4**, 302 (2009).
- ³⁴M. Geisler, R. R. Netz, and T. Hugel, *Angew. Chem. Int. Ed. Engl.* **49**, 4730 (2010).
- ³⁵A. Garg and S. B. Sinnott, *Phys. Rev. B* **60**, 13786 (1999).
- ³⁶A. Kutana, K. P. Giapis, J. Y. Chen, and C. P. Collier, *Nano Lett.* **6**, 1669 (2006).
- ³⁷M. C. Strus and A. Raman, *Phys. Rev. B* **80**, 224105 (2009).
- ³⁸L. Qu, L. Dai, M. Stone, Z. Xia, and Z. L. Wang, *Science* **322**, 238 (2008).
- ³⁹L. Ge, S. Sethi, L. Ci, P. M. Ajayan, and A. Dhinojwala, *Proc. Natl. Acad. Sci. USA* **104**, 10792 (2007).
- ⁴⁰K. Autumn, M. Sitti, Y. A. Liang, A. M. Peattie, W. R. Hansen, S. Sponberg, T. W. Kenny, R. Fearing, J. N. Israelachvili, and R. J. Full, *Proc. Natl. Acad. Sci. USA* **99**, 12252 (2002).
- ⁴¹H. Dai, J. H. Hafner, A. G. Rinzler, D. T. Colbert, and R. E. Smalley, *Nature (London)* **384**, 147 (1996).
- ⁴²J. H. Hafner, C. L. Cheung, and C. M. Lieber, *Nature (London)* **398**, 761 (1999).
- ⁴³J. H. Hafner, C. L. Cheung, A. T. Woolley, and C. M. Lieber, *Prog. Biophys. Mol. Biol.* **77**, 73 (2001).
- ⁴⁴S. I. Lee, S. W. Howell, A. Raman, R. Reifengerger, C. V. Nguyen, and M. Meyyappan, *Nanotechnology* **15**, 416 (2004).
- ⁴⁵N. R. Wilson and J. V. Macpherson, *Nat. Nanotech.* **4**, 483 (2009).
- ⁴⁶R. M. Stevens, *Mater. Today* **12**, 42 (2009).
- ⁴⁷Y. V. Shtogun and L. M. Woods, *J. Phys. Chem. Lett.* **1**, 1356 (2010).
- ⁴⁸C. Bernard, S. Marsaudon, R. Boisgard, and J.-P. Aimé, *Nanotechnology* **19**, 035709 (2008).
- ⁴⁹J. N. Israelachvili, *Intermolecular and Surface Forces* (Academic, London, 1992).
- ⁵⁰M. C. Strus, C. I. Cano, R. B. Pipes, C. V. Nguyen, and A. Raman, *Compos. Sci. Technol.* **69**, 1580 (2009).
- ⁵¹C. González, J. Ortega, F. Flores, D. Martínez-Martín, and J. Gómez-Herrero, *Phys. Rev. Lett.* **102**, 106801 (2009).
- ⁵²A. Kis, G. Csányi, J.-P. Salvetat, T.-N. Lee, E. Couteau, A. J. Kulik, W. Benoit, J. Brugger, and L. Forró, *Nat. Mater.* **3**, 153 (2004).
- ⁵³L. A. Chtcheglova, G. T. Shubeita, S. K. Sekatskii, and G. Dietler, *Biophys. J.* **86**, 1177 (2004).
- ⁵⁴Y. Zhang, C. Liu, W. Shi, Z. Wang, L. Dai, and X. Zhang, *Langmuir* **23**, 7911 (2007).
- ⁵⁵M. Seydou, S. Marsaudon, J. Buchoux, J.-P. Aimé, and A. M. Bonnot, *Phys. Rev. B* **80**, 245421 (2009).
- ⁵⁶A. Szabados, L. P. Biró, and P. R. Surján, *Phys. Rev. B* **73**, 195404 (2006).
- ⁵⁷L. A. Girifalco and R. A. Lad, *J. Chem. Phys.* **25**, 693 (1956).
- ⁵⁸P. A. Gravil, M. Devel, P. Lambin, X. Bouju, C. Girard, and A. A. Lucas, *Phys. Rev. B* **53**, 1622 (1996).
- ⁵⁹I. C. Gerber and J. G. Ángyán, *Chem. Phys. Lett.* **416**, 370 (2005).
- ⁶⁰J. G. Ángyán, I. C. Gerber, A. Savin, and J. Toulouse, *Phys. Rev. A* **72**, 012510 (2005).
- ⁶¹D. C. Langreth, M. Dion, H. Rydberg, E. Schröder, P. Hyldgaard, and B. I. Lundqvist, *Int. J. Quantum Chem.* **101**, 599 (2005).
- ⁶²H. Rydberg, M. Dion, N. Jacobson, E. Schröder, P. Hyldgaard, S. I. Simak, D. C. Langreth, and B. I. Lundqvist, *Phys. Rev. Lett.* **91**, 126402 (2003).
- ⁶³Y. J. Dappe, M. A. Basanta, F. Flores, and J. Ortega, *Phys. Rev. B* **74**, 205434 (2006).
- ⁶⁴Y. J. Dappe, J. Ortega, and F. Flores, *Phys. Rev. B* **79**, 165409 (2009).
- ⁶⁵L. Marty, V. Bouchiat, C. Naud, M. Chaumont, T. Fournier, and A. M. Bonnot, *Nano Lett.* **3**, 1115 (2003).
- ⁶⁶L. Marty, A. Iaia, M. Faucher, V. Bouchiat, C. Naud, M. Chaumont, T. Fournier, and A.-M. Bonnot, *Thin Solid Films* **501**, 299 (2006).
- ⁶⁷A. Loiseau, J. Gavillet, F. Ducastelle, J. Thibault, O. Stéphan, P. Bernier, and S. Thair, *C. R. Phys.* **4**, 975 (2003).
- ⁶⁸J. Gavillet, J. Thibault, O. Stéphan, H. Amara, A. Loiseau, C. Bichara, J.-P. Gaspard, and F. Ducastelle, *J. Nanosci. Nanotechnol.* **4**, 346 (2004).
- ⁶⁹M. A. Basanta, Y. J. Dappe, J. Ortega, and F. Flores, *Europhys. Lett.* **70**, 355 (2005).
- ⁷⁰G. Savini, Y. J. Dappe, S. Öberg, J. C. Charlier, M. I. Katsnelson, and A. Fasolino, *Carbon* **49**, 62 (2011).
- ⁷¹J. P. Lewis, K. R. Glaesemann, G. A. Voth, J. Fritsch, A. A. Demkov, J. Ortega, and O. F. Sankey, *Phys. Rev. B* **64**, 195103 (2001).
- ⁷²O. F. Sankey and D. J. Niklewski, *Phys. Rev. B* **40**, 3979 (1989).
- ⁷³A. A. Demkov, J. Ortega, O. F. Sankey, and M. P. Grumbach, *Phys. Rev. B* **52**, 1618 (1995).
- ⁷⁴P. Jelínek, H. Wang, J. P. Lewis, O. F. Sankey, and J. Ortega, *Phys. Rev. B* **71**, 235101 (2005).
- ⁷⁵M. A. Basanta, Y. J. Dappe, P. Jelínek, and J. Ortega, *Comput. Mater. Sci.* **39**, 759 (2007).
- ⁷⁶N. Troullier and J. L. Martins, *Solid State Commun.* **74**, 613 (1990).
- ⁷⁷N. Troullier and J. L. Martins, *Phys. Rev. B* **43**, 1993 (1991).
- ⁷⁸T. Hertel, R. E. Walkup, and P. Avouris, *Phys. Rev. B* **58**, 13870 (1998).
- ⁷⁹J. Mahanty and B. W. Ninham, *Dispersion Forces* (Academic, London, 1976).
- ⁸⁰R. Esquivel-Sirvent, *J. Chem. Phys.* **132**, 194707 (2010).
- ⁸¹M. C. Strus, L. Zalamea, A. Raman, R. B. Pipes, C. V. Nguyen, and E. A. Stach, *Nano Lett.* **8**, 544 (2008).